



**HAL**  
open science

## Anti-correlation phenomena in quantum cascade laser frequency combs

Baptiste Chomet, Tecla Gabbrielli, D. Gacemi, Francesco Cappelli, Luigi Consolino, Paolo de Natale, Filippos Kapsalidis, Angela Vasanelli, Y. Todorov, Jerome Faist, et al.

### ► To cite this version:

Baptiste Chomet, Tecla Gabbrielli, D. Gacemi, Francesco Cappelli, Luigi Consolino, et al.. Anti-correlation phenomena in quantum cascade laser frequency combs. *APL Photonics*, 2023, 8 (10), pp.106106. 10.1063/5.0160103. hal-04782377

**HAL Id: hal-04782377**

**<https://hal.science/hal-04782377v1>**

Submitted on 14 Nov 2024

**HAL** is a multi-disciplinary open access archive for the deposit and dissemination of scientific research documents, whether they are published or not. The documents may come from teaching and research institutions in France or abroad, or from public or private research centers.

L'archive ouverte pluridisciplinaire **HAL**, est destinée au dépôt et à la diffusion de documents scientifiques de niveau recherche, publiés ou non, émanant des établissements d'enseignement et de recherche français ou étrangers, des laboratoires publics ou privés.



Distributed under a Creative Commons Attribution 4.0 International License

RESEARCH ARTICLE | OCTOBER 17 2023

# Anti-correlation phenomena in quantum cascade laser frequency combs <sup>EP</sup>

B. Chomet <sup>ID</sup> ; T. Gabbriellini <sup>ID</sup> ; D. Gacemi <sup>ID</sup> ; F. Cappelli <sup>ID</sup> ; L. Consolino <sup>ID</sup> ; P. De Natale <sup>ID</sup> ; F. Kapsalidis <sup>ID</sup> ; A. Vasanelli <sup>ID</sup> ; Y. Todorov <sup>ID</sup> ; J. Faist <sup>ID</sup> ; C. Sirtori <sup>ID</sup>



APL Photonics 8, 106106 (2023)  
<https://doi.org/10.1063/5.0160103>



View Online



Export Citation

## Articles You May Be Interested In

Modeling of fluctuations in dynamical optoelectronic device simulations within a Maxwell-density matrix Langevin approach

Self-consistent simulations of intracavity terahertz comb difference frequency generation by mid-infrared quantum cascade lasers

*J. Appl. Phys.* (June 2023)

*In vivo* label-free tissue histology through a microstructured imaging window

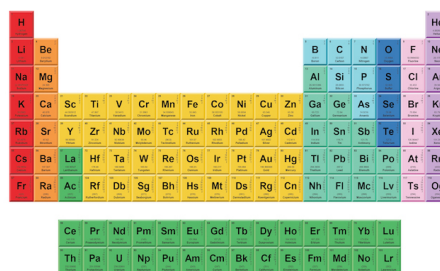
*APL Bioeng.* (January 2024)

14 November 2024 10:07:43



THE MATERIALS SCIENCE MANUFACTURER®

Now Invent.™



American Elements  
 Opens a World of Possibilities

...Now Invent!

[www.americanelements.com](http://www.americanelements.com)

© 2021-2024 American Elements & U.S. Registered Trademark

# Anti-correlation phenomena in quantum cascade laser frequency combs

Cite as: APL Photon. 8, 106106 (2023); doi: 10.1063/5.0160103

Submitted: 30 May 2023 • Accepted: 27 September 2023 •

Published Online: 17 October 2023



View Online



Export Citation



CrossMark

B. Chomet,<sup>1</sup>  T. Gabbrielli,<sup>2,3</sup>  D. Gacemi,<sup>1</sup>  F. Cappelli,<sup>2,3</sup>  L. Consolino,<sup>2,3</sup>  P. De Natale,<sup>2,3</sup>   
F. Kapsalidis,<sup>4</sup>  A. Vasanelli,<sup>1</sup>  Y. Todorov,<sup>1</sup>  J. Faist,<sup>4</sup>  and C. Sirtori<sup>1</sup> 

## AFFILIATIONS

<sup>1</sup>Laboratoire de Physique de l'Ecole normale supérieure, ENS, Université PSL, CNRS, Sorbonne Université, Université Paris Cité, Paris, France

<sup>2</sup>CNR-INO—Istituto Nazionale di Ottica, Via Carrara, 1–50019 Sesto Fiorentino, FI, Italy

<sup>3</sup>LENS—European Laboratory for Non-Linear Spectroscopy, Via Carrara, 1–50019 Sesto Fiorentino, FI, Italy

<sup>4</sup>Institute for Quantum Electronics, ETH Zürich, Zürich, Switzerland

<sup>a)</sup> Author to whom correspondence should be addressed: [carlo.sirtori@ens.fr](mailto:carlo.sirtori@ens.fr)

## ABSTRACT

In quantum cascade laser frequency combs, the intensity distribution of the optical spectrum can be split into two well-separated lobes of longitudinal modes that, even when far apart, have a common phase relation and preserve equal frequency separation. The temporal dynamics of two lasers emitting at 4.4 and 8.1  $\mu\text{m}$  operating in this bilobed regime are here investigated. The laser intensity shows a peculiar temporal behavior associated with the spectral features whereby, every half a round-trip, the total emitted power switches from one lobe to the other, with a perfect temporal anti-correlation. The anti-correlation between the lobes is also observed in the intensity noise figure of the emission. This coherent phenomenon arises from gain nonlinearities induced by spatial hole burning and the extremely fast gain dynamics typical of quantum cascade lasers.

© 2023 Author(s). All article content, except where otherwise noted, is licensed under a Creative Commons Attribution (CC BY) license (<http://creativecommons.org/licenses/by/4.0/>). <https://doi.org/10.1063/5.0160103>

## INTRODUCTION

Optical frequency combs<sup>1,2</sup> are sets of evenly spaced frequency modes that obey a well-defined phase relation. In the time domain, their intensity forms a perfectly periodic pattern, with a period corresponding to a photon roundtrip in the cavity. In the literature, frequency combs are mostly linked to mode-locked lasers that emit a train of short pulses. However, a comb spectrum can be associated with any periodic signal, regardless of its shape. A special case of interest is that of a perfectly constant intensity, where the periodicity is just given by the modulation of the carrier frequency. This extreme situation is very similar to that of frequency combs in quantum cascade lasers. Here, the phase relation between the modes is indeed imposed by a strong frequency modulation that spans, in a round trip, all the frequencies available in the gain bandwidth.<sup>3–5</sup> Recently, interest in the nonlinear dynamics of multi-mode quantum cascade lasers (QCLs) has progressively increased because their self-starting frequency modulated (FM) comb (QCL-comb)

emission is ideal for exploiting a wide spectral band within a single device. This feature within the spectral coverage of these devices (from mid- to far-infrared) makes QCL-combs a powerful tool for precise spectroscopic applications as well as for ultra-sensitive detection in multi-heterodyne configuration.<sup>6–8</sup> While some of the peculiar properties of QCL-combs, such as the frequency chirp operation and the parabolic distribution of the modal phases, have already been understood,<sup>9,10</sup> the presence of nonlinear interactions that set new dynamical phenomena, resulting from collective self-organization of the modes with unexpected temporal correlations, has recently emerged. For example, both correlation and anti-correlations in the intensity fluctuations of a harmonic QCL comb have been reported and have been linked to an effective Four Wave Mixing (FWM) process between the longitudinal modes.<sup>11</sup>

In this work, we report on the dynamics of two QCL combs emitting at 4.4 and 8.1  $\mu\text{m}$ , respectively, and exhibiting a spectrum made of two lobes of several longitudinal modes, separated by a large spectral gap ( $>15\text{ cm}^{-1}$  or 500 GHz). Such an optical spectrum is

typical of QCL emission when operated at a high bias current, as already reported in Refs. 8–13. Despite the spectral intensity gap, we show that the coherence of the comb is maintained across the entire gain spectrum. The modes of the two lobes beat and write a population density grating oscillating at very high frequencies in the gain medium with an instantaneous-like response. This grating couples the lobes and manifests itself in the temporal domain by switching between the two-lobe intensity and a periodicity at the laser cavity round trip time. This anti-phase behavior between the intensity of the two lobes is expected from the maximum emission principle,<sup>14</sup> which minimizes the gain fluctuations in order to keep the laser total output power constant. Moreover, the intensity fluctuations of each lobe are investigated in the RF frequency band below 100 MHz and are found to be anti-correlated.

**Characterization, results and discussion**

Our investigation focuses on combs originating from two QCLs with an active region made of strain-compensated dual-

stack heterostructure grown by molecular beam epitaxy emitting at  $\lambda = 4.4 \mu\text{m}$  and  $\lambda = 8.1 \mu\text{m}$ . The laser at  $4.4 \mu\text{m}$  ( $8.1 \mu\text{m}$ ) has a 4.5-mm (6-mm) long ridge resulting in a mode spacing of about 10 GHz (7.4 GHz) and corresponding to a photon round trip time in the cavity of  $T_{\text{rep}} = 100 \text{ ps}$  (140 ps). The two lasers are electrically injected with a low noise driver and a bias-T that sends the RF part of the current to a spectrum analyzer for measuring the inter-modal beat note. The two devices operate in a continuous wave at a fixed temperature (close to 265 K), stabilized by a low noise temperature controller (ppqSense, QubeCL). The evolution of the spectrum of the two devices as a function of the injected current is shown in Figs. 1(a) and 1(c). Starting from the laser threshold, the spectrum is almost single-mode; increasing the current results in more modes oscillating in the cavity with the spectrum eventually switching in the bilobed comb regime. Figures 1(b) and 1(d) show an example of the bilobed emission for each laser where the modal intensity is reduced by 20 dB in the spectral gap.

For comb formation, the dispersion has to exhibit a non-vanishing second order expansion, i.e., a significant group delay dispersion (GDD).<sup>9,10</sup> Notice that a spectrally flat GDD has been

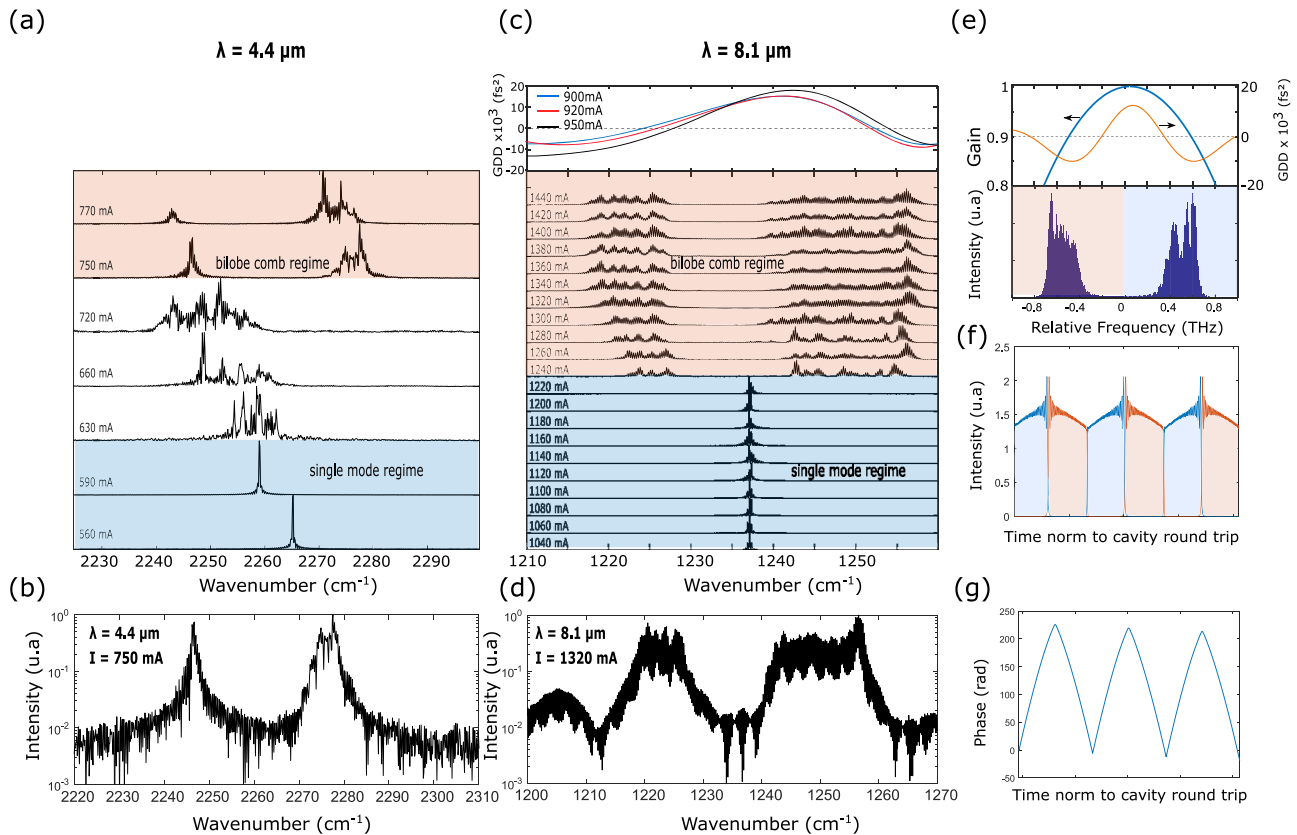


**FIG. 1.** (a) Optical spectra of the 4.5-mm QCL comb emitting at  $\lambda = 4.4 \mu\text{m}$  at 268 K. The QCL comb spectrum is centered at  $2262 \text{ cm}^{-1}$  and spans over  $35 \text{ cm}^{-1}$  in the bilobed comb regime. (b) Laser spectrum in log scale taken at the driving current  $I = 750 \text{ mA}$  showing a modal intensity reduction of over 20 dB inside the spectral gap. (c) Top: Measured second-order dispersion through analysis of the sub-threshold interferogram with an FTIR ( $0.2 \text{ cm}^{-1}$  resolution). Bottom: optical spectra of the 6-mm QCL comb emitting at  $\lambda = 8.1 \mu\text{m}$  at 263 K. The QCL comb spectrum is centered at  $1237 \text{ cm}^{-1}$  and spans over  $35 \text{ cm}^{-1}$  in the comb regime. (d) Laser spectrum in log scale taken at  $I = 1320 \text{ mA}$  showing a modal intensity reduction of over 20 dB inside the spectral gap. (e) Simulated (see Ref. 10) QCL optical spectrum in the case of a continuous gain spectrum and a spectrally dependent GDD reproduces the bilobed spectrum. (f) Simulation of the laser intensity over three cavity round trips showing the switching behavior between the intensity of the two lobes. (g) Phase of the field over three cavity round trips.

theoretically shown to produce an optical spectrum with modes of constant amplitude and a linear chirp of the optical frequency that comprises the whole laser spectrum. In a previous report, the Risken–Nummedal–Graham–Haken instability has been thought to be the main reason that separates the optical spectra into two groups of modes with a gap in between, as for the lasers here reported. However, in this model, the presence of an absorber in the cavity was required to reach such a regime.<sup>15</sup> We believe that the bilobed regime observed often in QCL combs is rather produced by a non-constant bell-shaped GDD, as we reported at the top of Fig. 1(c). This shape has been derived from Hakki-Paoli measurements of the gain below the threshold and is a consequence of the peak gain (see supplementary material, Appendix S1). By inserting the GDD on the top part of Fig. 1(c) into our mean-field simulations<sup>10</sup> of the QCL comb dynamics, we were able to reproduce the bilobed optical spectrum presented in Fig. 1(e). Following Ref. 10, the shape of the GDD stabilizes the frequency chirped operation of the laser on both minima, which leads to a discontinuous spectrum where each group of modes oscillates in anti-phase. These simulations show that the spectral dependence of the GDD has a significant impact on the laser spectrum. In this configuration, the laser enters a stable but peculiar operation in which the intensity of two lobes alternates in time: the laser emits, for the first half of a round trip, on the blue lobe and then switches, for the second half, on the red one. The mean field simulations are also able to reproduce this behavior, as illustrated in Fig. 1(f), where we plot each lobe intensity over three round trips of the corresponding bilobed spectrum. Here, we believe that the synchronization mechanisms between the two lobes are due

to the instantaneous-like response of the gain. As we have previously mentioned, the beating of different laser modes leads to oscillations of the carrier density in the gain medium, which, in turn, couples with the laser modes.<sup>16,17</sup> In QCLs, due to the inherent ultra-short relaxation time of the gain, this FWM process allows the locking of comb teeth even with spacing comparable to the gain recovery frequency.<sup>18</sup> The gain relaxation rate is still fast enough for the carriers to respond at the frequency difference between the two lobes, hence coupling them together. We have checked the validity of this ultrafast phenomenon through numerical simulations by forcing the intensity of oscillating modes to zero in the spectral gap of Fig. 1(f). Even in this extreme condition, the total intensity [Fig. 1(f)] and the phase [Fig. 1(g)] of the field are continuous despite the spectral gap, confirming that the coherence is transferred from one lobe to the other.

In the following, we measure the lasers' emission using two different techniques, the shifted-wave interference Fourier-transform spectroscopy (SWIFTS)<sup>5</sup> and Fourier analysis of comb emission (FACE).<sup>19</sup> We aim to prove that, despite the spectral gap, the separated spectral lobes belong to the same frequency comb.

Figure 2(a) shows the experimental setup of the SWIFTS. This technique allows us to retrieve the phase difference between adjacent modes, thus enabling the reconstruction of the temporal dependence of the intensity during one period of the comb. The characterization of the laser at  $\lambda = 4.4 \mu\text{m}$  is performed with a homemade interferometer equipped with a fast and sensitive Mercury–Cadmium–Telluride (MCT) detector (VIGO Photonics) to observe the laser beat-note at 10 GHz. For characterization at

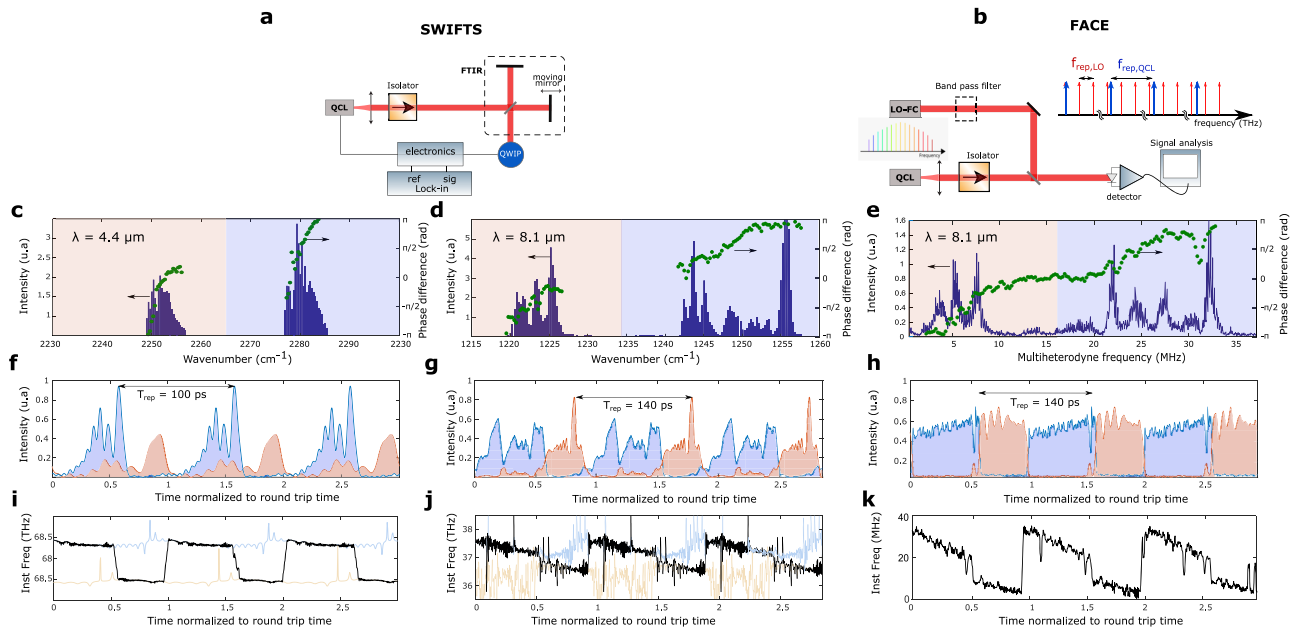


**FIG. 2.** (a) Experimental setup for the QCL time domain profile characterization using SWIFTS. (b) Experimental setup for the QCL time domain profile characterization using FACE. (c) SWIFTS reconstructed the intensity and intermodal phase difference of the laser emitting at  $\lambda = 4.4 \mu\text{m}$  for  $I = 765 \text{ mA}$  and (d) for the laser emitting at  $\lambda = 8.1 \mu\text{m}$  at  $I = 1280 \text{ mA}$ . (e) Reconstructed intensity and phase difference of the laser emitting at  $\lambda = 8.1 \mu\text{m}$  at  $I = 1280 \text{ mA}$  using FACE. (f)–(h) Reconstructed time evolution over three round trips of the intensity of each spectral lobe corresponding to the above spectrum. The time is normalized to the cavity round-trip time,  $T_{\text{rep}}$ . Pulse-like switching behavior is observed between the two spectral regions of the laser. (i)–(k) Instantaneous frequency of the laser emission over three round trips.

$\lambda = 8.1 \mu\text{m}$ , the laser light is sent through a Fourier transform infrared spectrometer (FTIR, resolution of  $0.2 \text{ cm}^{-1}$ ) onto a liquid nitrogen cooled quantum well infrared photodetector (QWIP). Figures 2(c) and 2(d) show the mode amplitude and intermodal phase retrieved with the SWIFTS. The latter is not constant over the spectrum but linear and spans over  $2\pi$ , which is characteristic of the linear frequency chirp behavior of the instantaneous laser frequency. In order to retrieve the laser emission profile, the phase relation of the spectrum is usually retrieved through a cumulative sum of the intermodal phase differences. Due to our finite signal-to-noise ratio, information about the latter is lost in the spectral gap, which obliges us to speculate on the phase difference between the two lobes (see supplementary material, Appendix S2). In order to confirm the swinging spectral dynamics, the temporal profile of the laser emitting at  $\lambda = 8.1 \mu\text{m}$  is directly measured using multi-heterodyne dual comb detection by beating on a high-speed detector the QCL-comb with a reference optical frequency comb as the Local Oscillator (LO-FC). The latter is a conventional mode locked laser that directly emits in the mid-infrared region spanning the  $7.4$  to  $9.4 \mu\text{m}$  spectral window (full-width-half-maximum FWHM  $\sim 4.29 \text{ THz}$ ), whose modes have all a constant phase

difference and are spaced by  $f_{\text{rep},\text{LO}} = 100 \text{ MHz}$ . The FACE experimental setup is shown in Fig. 2(b). To ensure the optical field in the THz domain to be down-converted in the MHz range, the Peltier temperature and the current of the QC laser are set such that the intermodal frequency spacing of the QC comb,  $f_{\text{rep},\text{QCL}} = 7.39 \text{ GHz}$ , satisfying the condition  $f_{\text{rep},\text{QCL}} = n f_{\text{rep},\text{LO}} + \delta f$ , with  $n$  being an integer and  $\delta f$  in the order of  $100 \text{ kHz}$ . The latter sets the mode spacing of the multi-heterodyne spectrum. The beating between the two combs on a high-speed detector (VIGO Photonics, PV-4TE-10.6,  $800 \text{ MHz}$  bandwidth) gives an interference pattern that can be used to retrieve the phase difference, through the entire spectrum, of the QCL under test.<sup>19</sup> To that end, the temporal signal at the output of the detector is acquired in the time domain on an oscilloscope with a sample rate of  $250 \text{ MS/s}$  over  $1 \text{ ms}$ . Fourier analysis of the temporal trace reveals the complex multi-heterodyne spectrum shown in Fig. 2(h) with a spectral resolution of  $10 \text{ kHz}$  (see supplementary material, Appendix S3).

The instantaneous laser intensity within three cavity round trips using SWIFTS and FACE is shown in Figs. 2(f)–2(h) and illustrates that the laser intensity is into the red lobe only when the blue lobe is off and vice versa. Yet, a small temporal overlap between the

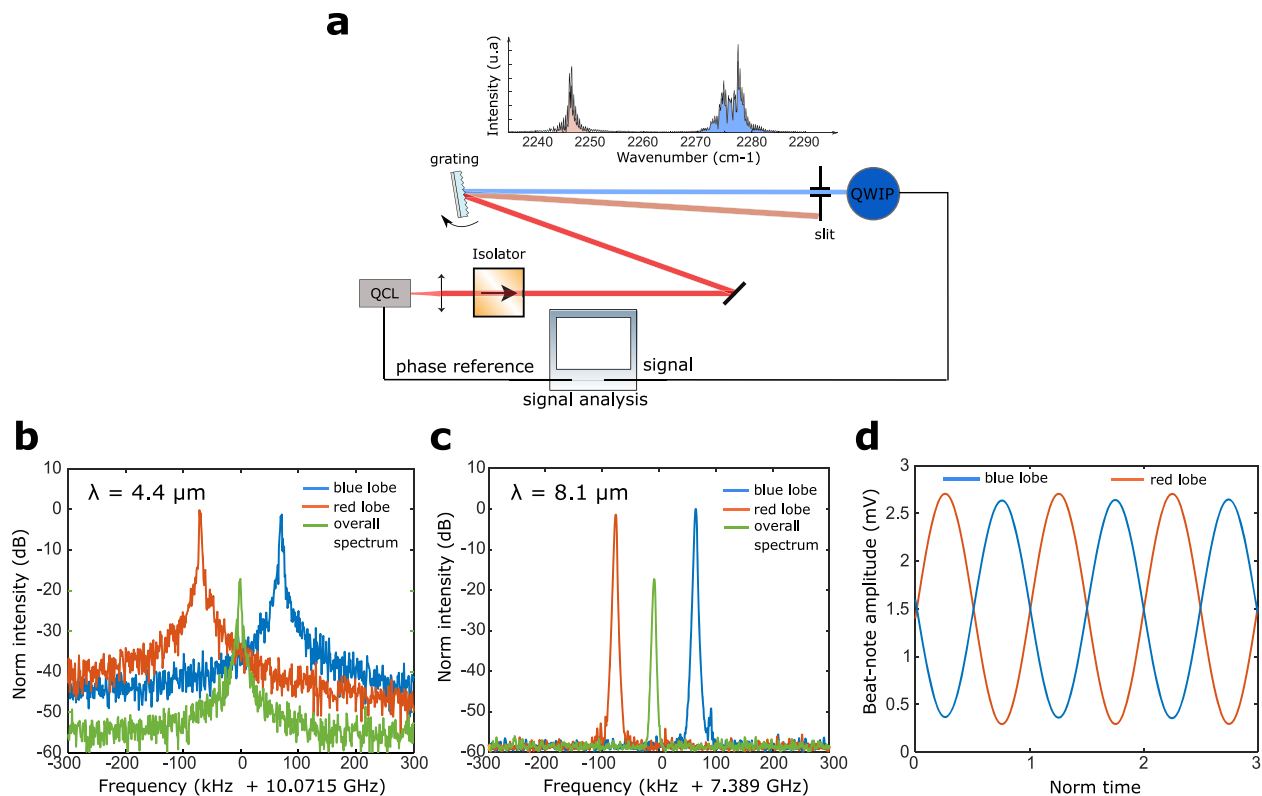


**FIG. 3.** (a) An example of the bilobed emission by the QCL-comb emitting at  $4.4 \mu\text{m}$  recorded at  $I = 765 \text{ mA}$  and a sketch of the experimental setup for beat-note measurements. The bilobed emission from the QCL comb is split by a grating resulting in two spatially separated beams. Each beam is sent one by one to a high speed detector (VIGO Photonics for the setup at  $4.4 \mu\text{m}$  and QWIP for the setup at  $8.1 \mu\text{m}$ ). (b) Optical beat notes for each spectral lobe and the overall spectrum for the laser at  $4.4 \mu\text{m}$  ( $200 \text{ Hz}$  resolution bandwidth) and (c) for the laser at  $8.1 \mu\text{m}$  ( $3 \text{ kHz}$  resolution bandwidth). The beat notes are frequency shifted to  $70 \text{ kHz}$  for the sake of clarity. (d) To acquire the optical beat notes in the time domain, the latter are down converted at the RF frequency  $137 \text{ MHz}$  with a local oscillator whose frequency is set at  $f_{\text{rep},\text{QCL}} - 137 \text{ MHz}$ . The electrical beat note is down converted with the same local oscillator and used as a phase reference.

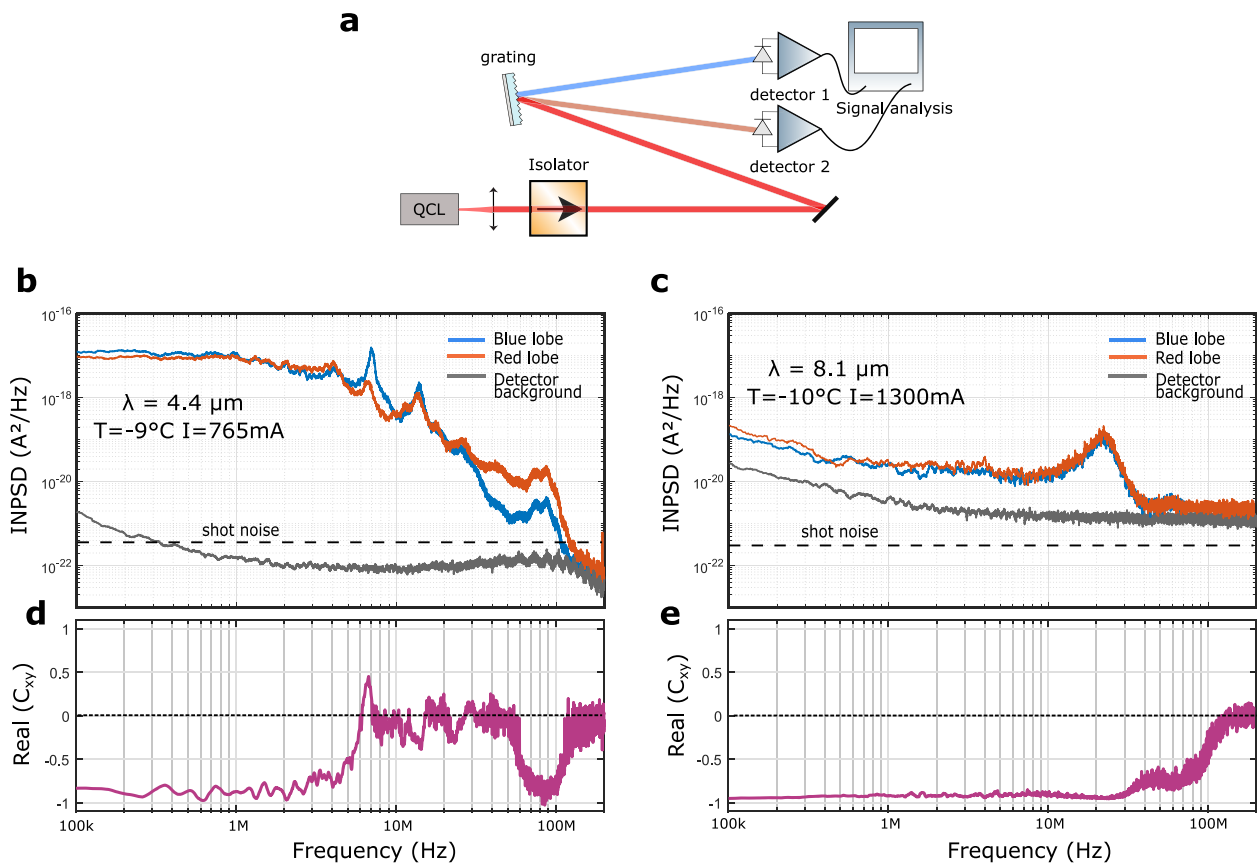


**FIG. 4.** (a) Experimental setup for correlation measurements. The bilobed emission from the QCL comb is split by a grating resulting in two spatially separated beams. Both beams are sent simultaneously to two similar high-speed detectors. Data analysis is performed digitally in post-production. (b) INPSD measurements of the two spectral lobes of the laser at  $4.4 \mu\text{m}$  for  $I = 765 \text{ mA}$ ,  $T = 264 \text{ K}$ , and (c) for the laser at  $8.1 \mu\text{m}$  for  $I = 1300 \text{ mA}$ ,  $T = 263 \text{ K}$ . (d) and (e) Real part of the correlation coefficient  $C_{\text{Lobe1,Lobe2}}$ .

two lobe intensities is apparent, which implies continuity of the total laser intensity. The instantaneous frequency of each lobe as well as the total field are shown in Figs. 2(i)–2(k). One can recognize a discontinuity in the instantaneous laser frequency, which confirms that no emission occurs in the spectral gap region.

A further proof of the dynamical behavior of the two spectral lobes of the QCL comb has been obtained with the setup depicted in Fig. 3(a), which provides direct information on their phase relation.

In this experiment, the two spectral lobes are spatially separated by means of a diffraction grating with a groove density of 150–300 grooves/mm, allowing the detection of each lobe individually on a fast detector. The intermodal beat note of each beam is shown in Figs. 3(b) and 3(c) for both lasers. Note that the peak frequency of the beat notes has been shifted by  $\pm 70 \text{ kHz}$  with respect to their central frequency for the sake of readability. Moreover, with this setup, it is also possible to record the overall laser intensity by rotating the grating and measuring the zero-order diffracted beam. We notice an

attenuation of  $-18 \text{ dB}$  of the overall modes beating compared to that in each lobe, in good agreement with the switching behavior of the laser and with the intensity of the overall spectrum, which is almost constant. Moreover, as the intermodal beat note is the first harmonic of the time-dependent intensity shown in Figs. 2(f)–2(h), we expect anti-phase behavior between the beat notes of each lobe. The electrical and optical beat notes, after amplification, are down-converted to  $137 \text{ MHz}$  using the same RF local oscillator operating at the frequency  $f_{\text{LO}} = f_{\text{rep,QCL}} - 137 \text{ MHz}$ . In order to set a phase reference, the detector signal from one diffracted beam is recorded simultaneously with the electrical beat note on two different channels of an oscilloscope. The time oscillations of the recorded beat notes (blue lobe and red lobe) are shown in Fig. 3(d), where the electrical beat note is used as a phase reference. As expected, the two beat notes coming from each lobe show close to perfect anti-phase behavior.

We now focus on the intensity fluctuations of each lobe and their correlations, detected here in a  $100 \text{ MHz}$  bandwidth. As demonstrated before, the two lobes are part of the same comb, and

correlations between their noise signatures can then be expected as in any mode locked laser. As described earlier, gain fluctuations will be reduced following the maximum emission principle. Since both spectral lobes share the same gain medium, the intensity fluctuations of one lobe will be counter balanced by the other. To show this, both beams are now sent simultaneously to two similar high-speed detectors, as shown in Fig. 4(a), each of which collects the optical power from a single lobe. The electrical signal at the output of each detector is acquired simultaneously in the time domain on a fast oscilloscope following Ref. 20.

Figures 4(b) and 4(c) show the intensity noise spectral density (INPSD) of the two spectral lobes of the laser emitting at  $4.4 \mu\text{m}$  ( $I = 765 \text{ mA}$ ,  $T = 264 \text{ K}$ ) and  $8.1 \mu\text{m}$  ( $I = 1300 \text{ mA}$ ,  $T = 263 \text{ K}$ ). The two spectral lobes display similar intensity fluctuations in a 100 MHz bandwidth, which is much smaller than the frequency difference between two consecutive modes. The shot noise level as well as the detector background noise are also indicated. Figure 4(b) reveals that the measurement is shot noise limited, but the large intensity fluctuations and the 120 MHz cutoff of the detector do not allow us to investigate the noise properties for higher frequencies. The 10-MHz cutoff in the spectra is due to internal dynamics inherent to frequency-comb generation in QCLs.<sup>11</sup> On the other hand, for detection at  $8.1 \mu\text{m}$  [Fig. 4(c)], the intensity noise of the laser is lower, but the setup is not shot noise limited. Yet, simultaneous measurements of the time traces allow us to investigate the correlation properties between the fluctuations of the two lobes. One can define a complex correlation coefficient

$$C_{Lobe1,Lobe2} = \frac{INPSD_{Lobe1,Lobe2}}{\sqrt{INPSD_{Lobe1}INPSD_{Lobe2}}},$$

where  $INPSD_{Lobe1}$ , ( $INPSD_{Lobe2}$ ) represents the intensity noise power spectral density of the low (high) spectral components of the comb and  $INPSD_{Lobe1,Lobe2}$  the cross spectrum of the high and low components of the comb, which is the frequency analysis of the cross-correlation between the two time traces.<sup>21</sup> The absolute value of this quantity is equal to 1 when the two signals are identical apart from a time shift. When the two lobes are independent, the normalized correlation coefficient falls to zero. The normalized correlation coefficient extracted from our measurements at  $4.4$  and  $8.1 \mu\text{m}$  is presented in Figs. 4(d) and 4(e). The real part of the correlation coefficient is very close to  $-1$  and suggests an almost perfect anti-correlation behavior between the fluctuations of the two lobes up to  $\sim 100$  MHz. This is the result of both lobes sharing the same gain medium while being coupled with each other's through non-linear mixing. Above this frequency,  $C_{Lobe1,Lobe2}$  quickly goes to zero since the level of noise decreases to the detector background noise level. Regarding the lack of anti-correlation between  $\sim 6$  and  $60$  MHz in the  $\lambda = 4.4 \mu\text{m}$  QCL emission, we believe it is due to an excess of noise present in one of the two lobes arising from an internal dynamics.

## CONCLUSION

We have studied the emission properties of two QCL frequency combs whose optical spectrum is composed of two sets of longitudinal modes (lobes). Analysis of the intermodal phases reveals a switching behavior between the intensity of the two spectral lobes within a round-trip. Such dynamics is triggered by an efficient

FWM process and spatial hole burning that strongly couple the modes to minimize the laser's overall intensity fluctuations. We have shown that this phenomenon is apparent within one round trip of the cavity together with an anti-correlation in the intensity noise of each lobe. Interestingly, FWM is also able to induce non-classical intensity correlations among the different modes, which have already been observed in other photonic devices such as optical fibers and microresonators.<sup>22–25</sup> Even if entanglement and quantum correlations have not yet been verified, we did demonstrate the existence of strong classical correlations in the intensity noise of QCLs. While the noise reported here is well above the shot noise level, the dynamical behavior concerning QCL comb intensity correlations described in this work can pave the way for a deeper understanding of the key parameters connected to the laser dynamics and frequency comb formation (e.g., the gain nonlinearities) to be optimized in view of promoting the fabrication of a new generation of QCLs optimized for a possible MIR direct non-classical light generation (e.g., squeezed light).

## SUPPLEMENTARY MATERIAL

See supplementary material for supporting content.

## ACKNOWLEDGMENTS

The authors acknowledge financial support by the ENS-Thales Chair and the European Union's Horizon 2020 Research and Innovation Program (Qombs Project, FET Flagship on Quantum Technologies Grant No. 820419; Laserlab-Europe Project Grant No. 871124; MUQUABIS Project Grant No. 101070546), the European Union's QuantERA II (Grant No. 101017733, QATACOMB Project), the European Union's NextGenerationEU Program, I-PHOQS Infrastructure (IR0000016, ID D2B8D520, CUP B53C22001750006), and the Ile-de-France Region in the framework of DIM SIRTEQ.

## AUTHOR DECLARATIONS

### Conflict of Interest

The authors have no conflicts to disclose.

### Author Contributions

**B. Chomet:** Data curation (equal); Investigation (equal); Writing – original draft (equal); Writing – review & editing (equal). **T. Gabbrielli:** Data curation (equal); Investigation (equal); Writing – review & editing (equal). **D. Gacemi:** Writing – review & editing (supporting). **F. Cappelli:** Data curation (equal); Investigation (equal); Writing – review & editing (equal). **L. Consolino:** Writing – review & editing (supporting). **P. De Natale:** Writing – review & editing (equal). **F. Kapsalidis:** Resources (equal). **A. Vasanelli:** Writing – review & editing (supporting). **Y. Todorov:** Writing – review & editing (supporting). **J. Faist:** Writing – review & editing (equal). **C. Sirtori:** Investigation (equal);

Supervision (lead); Writing – original draft (equal); Writing – review & editing (equal).

## DATA AVAILABILITY

The data that support the findings of this study are available from the corresponding author upon reasonable request.

## REFERENCES

- <sup>1</sup>T. W. Hänsch, “Nobel lecture: Passion for precision,” *Rev. Mod. Phys.* **78**(4), 1297 (2006).
- <sup>2</sup>J. L. Hall, “Nobel Lecture: Defining and measuring optical frequencies,” *Rev. Mod. Phys.* **78**(4), 1279 (2006).
- <sup>3</sup>M. Singleton, P. Jouy, M. Beck, and J. Faist, “Evidence of linear chirp in mid-infrared quantum cascade lasers,” *Optica* **5**(8), 948–953 (2018).
- <sup>4</sup>J. Hillbrand, D. Auth, M. Piccardo, N. Opačak, E. Gornik, G. Strasser, F. Capasso, S. Breuer, and B. Schwarz, “In-phase and anti-phase synchronization in a laser frequency comb,” *Phys. Rev. Lett.* **124**(2), 023901 (2020).
- <sup>5</sup>D. Burghoff, Y. Yang, D. J. Hayton, J.-R. Gao, J. L. Reno, and Q. Hu, “Evaluating the coherence and time-domain profile of quantum cascade laser frequency combs,” *Opt. Express* **23**(2), 1190–1202 (2015).
- <sup>6</sup>L. Consolino, F. Cappelli, M. S. de Cumis, and P. De Natale, “QCL-based frequency metrology from the mid-infrared to the THz range: A review,” *Nanophotonics* **8**(2), 181–204 (2019).
- <sup>7</sup>S. Borri, G. Insero, G. Santambrogio, D. Mazzotti, F. Cappelli, I. Galli, G. Galzerano, M. Marangoni, P. Laporta, V. Di Sarno, L. Santamaria, P. Maddaloni, and P. De Natale, “High-precision molecular spectroscopy in the mid-infrared using quantum cascade lasers,” *Appl. Phys. B* **125**(1), 18 (2019).
- <sup>8</sup>G. Villares, A. Hugi, S. Blaser, and J. Faist, “Dual-comb spectroscopy based on quantum-cascade-laser frequency combs,” *Nat. Commun.* **5**(1), 5192 (2014).
- <sup>9</sup>N. Opačak and B. Schwarz, “Theory of frequency-modulated combs in lasers with spatial hole burning, dispersion, and Kerr nonlinearity,” *Phys. Rev. Lett.* **123**(24), 243902 (2019).
- <sup>10</sup>D. Burghoff, “Unraveling the origin of frequency modulated combs using active cavity mean-field theory,” *Optica* **7**(12), 1781–1787 (2020).
- <sup>11</sup>T. Gabbriellini, N. Bruno, N. Corrias, S. Borri, L. Consolino, M. Bertrand, M. Shahmohammadi, M. Franckić, M. Beck, J. Faist, A. Zavatta, F. Cappelli, and P. De Natale, “Intensity correlations in quantum cascade laser harmonic frequency combs,” *Adv. Photonics Res.* **3**, 2200162 (2022).
- <sup>12</sup>P. Täschler, M. Bertrand, B. Schneider, M. Singleton, P. Jouy, F. Kapsalidis, M. Beck, and J. Faist, “Femtosecond pulses from a mid-infrared quantum cascade laser,” *Nat. Photonics* **15**(12), 919–924 (2021).
- <sup>13</sup>J. Faist, G. Villares, G. Scalari, M. Rösch, C. Bonzon, A. Hugi, and M. Beck, “Quantum cascade laser frequency combs,” *Nanophotonics* **5**(2), 272–291 (2016).
- <sup>14</sup>C. L. Tang and H. Statz, “Maximum-emission principle and phase locking in multimode lasers,” *J. Appl. Phys.* **38**(7), 2963–2968 (1967).
- <sup>15</sup>A. Gordon, C. Y. Wang, L. Diehl, F. X. Kärtner, A. Belyanin, D. Bour, S. Corzine, G. Höfler, H. C. Liu, H. Schneider, T. Maier, M. Troccoli, J. Faist, and F. Capasso, “Multimode regimes in quantum cascade lasers: From coherent instabilities to spatial hole burning,” *Phys. Rev. A* **77**(5), 053804 (2008).
- <sup>16</sup>G. P. Agrawal, “Population pulsations and nondegenerate four-wave mixing in semiconductor lasers and amplifiers,” *J. Opt. Soc. Am. B* **5**(1), 147–159 (1988).
- <sup>17</sup>I. McMackin, C. Radzewicz, M. Beck, and M. G. Raymer, “Instabilities and chaos in a multimode, standing-wave, cw dye laser,” *Phys. Rev. A* **38**(2), 820–832 (1988).
- <sup>18</sup>D. Kazakov, M. Piccardo, Y. Wang, P. Chevalier, T. S. Mansuripur, F. Xie, C. Zah, K. Lascola, A. Belyanin, and F. Capasso, “Self-starting harmonic frequency comb generation in a quantum cascade laser,” *Nat. Photonics* **11**(12), 789–792 (2017).
- <sup>19</sup>F. Cappelli, L. Consolino, G. Campo, I. Galli, D. Mazzotti, A. Campa, M. Siciliani de Cumis, P. Cancio Pastor, R. Eramo, M. Rösch, M. Beck, G. Scalari, J. Faist, P. De Natale, and S. Bartalini, “Retrieval of phase relation and emission profile of quantum cascade laser frequency combs,” *Nat. Photonics* **13**(8), 562–568 (2019).
- <sup>20</sup>T. Gabbriellini, F. Cappelli, N. Bruno, N. Corrias, S. Borri, P. De Natale, and A. Zavatta, “Mid-infrared homodyne balanced detector for quantum light characterization,” *Opt. Express* **29**(10), 14536–14547 (2021).
- <sup>21</sup>F. W. King, *Hilbert Transforms* (Cambridge University Press, Cambridge, 2009).
- <sup>22</sup>H. P. Yuen and J. H. Shapiro, “Generation and detection of two-photon coherent states in degenerate four-wave mixing,” *Opt. Lett.* **4**(10), 334–336 (1979).
- <sup>23</sup>M. D. Levenson, R. M. Shelby, A. Aspect, M. Reid, and D. F. Walls, “Generation and detection of squeezed states of light by nondegenerate four-wave mixing in an optical fiber,” *Phys. Rev. A* **32**(3), 1550 (1985).
- <sup>24</sup>C. F. McCormick, V. Boyer, E. Arimondo, and P. D. Lett, “Strong relative intensity squeezing by four-wave mixing in rubidium vapor,” *Opt. Lett.* **32**(2), 178–180 (2007).
- <sup>25</sup>A. Dutt, K. Luke, S. Manipatruni, A. L. Gaeta, P. Nussenzveig, and M. Lipson, “On-chip optical squeezing,” *Phys. Rev. Appl.* **3**(4), 044005 (2015).